

in the coordination chemistry of silver and produces no appreciable instability in the compound.

All these factors may contribute to various degrees to the stability of the structure observed here.

Acknowledgment. We wish to thank the National Research Council of Canada and the Ministère de l'Éducation du Québec for financial support. We are very grateful to Dr. F. Rochon for permission to use the Syntex diffractometer and valuable assistance during data collection.

Registry No. [(adeninium)₂Ag₂](ClO₄)₄·H₂O, 63301-89-3.

Supplementary Material Available: Listings of structure factor amplitudes and H atom coordinates and a drawing showing the shape and dimensions of the crystal used (12 pages). Ordering information is given on any current masthead page.

References and Notes

- (1) C. Gagnon and A. L. Beauchamp, *Inorg. Chim. Acta*, **14**, L52 (1975); *Acta Crystallogr., Sect. B*, **33**, 1448 (1977).
- (2) G. H. Stout and L. H. Jensen, "X-Ray Structure Analysis", Macmillan, New York, N.Y., 1968, pp 420, 457.
- (3) W. H. Zachariassen, *Acta Crystallogr.*, **16**, 1139 (1963).
- (4) D. T. Cromer and J. T. Waber, *Acta Crystallogr.*, **18**, 104 (1965).
- (5) J. Stewart, R. Davidson, and A. Simpson, *J. Chem. Phys.*, **42**, 3175 (1965).
- (6) D. T. Cromer, *Acta Crystallogr.*, **18**, 17 (1965).
- (7) M. Authier-Martin and A. L. Beauchamp, *Can. J. Chem.*, **55**, 1213 (1977).
- (8) P. F. Lindley and P. Woodward, *J. Chem. Soc. A*, 123 (1966); C. S. Gibbons and J. Trotter, *ibid.*, 2058 (1971).
- (9) C. J. Gilmore, P. A. Tucker, S. F. Watkins, and P. Woodward, *Chem. Commun.*, 1006 (1969).
- (10) J. K. H. Rao and H. A. Viswamitra, *Acta Crystallogr., Sect. B*, **28**, 1484 (1972).
- (11) C. J. Antti and K. S. Lundberg, *Acta Chem. Scand.*, **25**, 1758 (1971); C. B. Acland and H. C. Freeman, *Chem. Commun.*, 1016 (1971).
- (12) R. G. Vranka and E. L. Amma, *Inorg. Chem.*, **5**, 1020 (1966).
- (13) R. L. Bodner and A. I. Popov, *Inorg. Chem.*, **11**, 1410 (1972); J. E. Fleming and H. Lynton, *Can. J. Chem.*, **46**, 471 (1968); R. H. Benno and C. J. Fritchie, *Acta Crystallogr., Sect. B*, **29**, 2493 (1973).
- (14) J. Cooper and R. E. Marsh, *Acta Crystallogr.*, **14**, 202 (1961).
- (15) "International Tables of X-Ray Crystallography", Vol. 3, Kynoch Press, Birmingham, England, 1968, p 278.
- (16) P. DeMeester and A. C. Skapski, *J. Chem. Soc., Dalton Trans.*, 2400 (1972).
- (17) A. Terzis, A. L. Beauchamp, and R. Rivest, *Inorg. Chem.*, **12**, 1166 (1973).
- (18) W. C. Hamilton and J. A. Ibers, "Hydrogen Bonding in Solids", W. A. Benjamin, New York, N.Y., 1968, p 16.
- (19) E. Sletten and B. Thorstensen, *Acta Crystallogr., Sect. B*, **30**, 2438 (1974); E. Sletten and M. Ruud, *ibid.*, **31**, 982 (1975).
- (20) A. Terzis, *Inorg. Chem.*, **15**, 793 (1976).
- (21) M. J. McCall and M. R. Taylor, *Acta Crystallogr., Sect. B*, **32**, 1687 (1976); P. DeMeester, D. M. L. Goodgame, A. Skapski, and Z. Warnke, *Biochim. Biophys. Acta*, **324**, 301 (1973).
- (22) M. J. McCall and M. R. Taylor, *Biochim. Biophys. Acta*, **390**, 137 (1975).
- (23) M. R. Taylor, *Acta Crystallogr., Sect. B*, **29**, 884 (1973).
- (24) G. M. Brown, *Acta Crystallogr., Sect. B*, **25**, 1338 (1969); E. Sletten, J. Sletten, and L. H. Jensen, *ibid.*, **25**, 1330 (1969).
- (25) P. Lavertue, J. Hubert, and A. L. Beauchamp, *Inorg. Chem.*, **15**, 322 (1976).
- (26) P. DeMeester and A. C. Skapski, *J. Chem. Soc. A*, 2167 (1971).
- (27) P. DeMeester and A. C. Skapski, *J. Chem. Soc., Dalton Trans.*, 424, 1596 (1973).
- (28) E. Sletten, *Acta Crystallogr., Sect. B*, **25**, 1480 (1969).
- (29) P. DeMeester, S. R. Fletcher, and A. C. Skapski, *J. Chem. Soc., Dalton Trans.*, 2575 (1973); G. M. Brown and R. Chidambaram, *Acta Crystallogr., Sect. B*, **29**, 2393 (1973).
- (30) R. G. Griffin, J. D. Ellett, M. Mehring, J. G. Bullitt, and J. S. Waugh, *J. Chem. Phys.*, **57**, 2147 (1972).
- (31) F. A. Cotton, B. G. DeBoer, M. D. LaPrade, J. R. Pipal, and D. A. Ucko, *Acta Crystallogr., Sect. B*, **27**, 1664 (1971); D. Lawton and R. Mason, *J. Am. Chem. Soc.*, **87**, 921 (1965); F. A. Cotton and J. G. Norman, *J. Coord. Chem.*, **1**, 161 (1971); M. J. Bennett, K. G. Caulton, and F. A. Cotton, *Inorg. Chem.*, **8**, 1 (1969); M. J. Bennett, W. K. Bratton, F. A. Cotton, and W. R. Robinson, *ibid.*, **7**, 1570 (1968).
- (32) P. Jennische and R. Hesse, *Acta Chem. Scand.*, **25**, 423 (1971).

Contribution from the Los Alamos Scientific Laboratory,
University of California, Los Alamos, New Mexico 87545

Novel Sulfur Dioxide Coordination in Nitrosyl(sulfur dioxide)bis(triphenylphosphine)rhodium and an Oxygen-18 Study of Its Reaction with Molecular Oxygen¹

DAVID C. MOODY* and R. R. RYAN*

Received March 16, 1977

AIC70199D

Crystals of Rh(NO)(SO₂)(PPh₃)₂ have been obtained from SO₂-saturated solutions of Rh(NO)(PPh₃)₃, and the structure has been determined at 25 °C. The compound crystallizes in the orthorhombic space group *Pbca* with *a* = 10.338 (2) Å, *b* = 18.500 (4) Å, *c* = 33.933 (7) Å, *d*_c = 1.48 g cm⁻³, *d*_m = 1.47 g cm⁻³, and *Z* = 8 (Cu Kα₁ radiation, λ 1.54051 Å). The structure refined to an unweighted *R* value of 0.038 for 2615 reflections with *I* > 2σ(*I*). The SO₂ binds to the metal both through the sulfur atom and through one oxygen atom with a Rh-S distance of 2.326 (2) Å and a Rh-O(2) distance of 2.342 (5) Å. The S-O(2) distance of 1.493 (5) Å is considerably longer than the S-O(1) distance of 1.430 (5) Å, while the O(1)-S-O(2) angle is 115.1 (4)°. The RhNO unit in this structure is clearly bent with a Rh-NO angle of 140.4 (6)°. The factors influencing the bending of the nitrosyl are discussed in terms of the metal coordination geometry and number of d electrons. The mechanism of the reaction of this S,O-bonded SO₂ with molecular oxygen to form coordinated sulfate has been studied utilizing oxygen-18 substitution and infrared analysis. This study has revealed a distribution of the labeled oxygen in the resulting Rh(NO)(SO₄)(PPh₃)₂ different from that observed for S-bonded SO₂ reactions with molecular oxygen.

Introduction

It is well established that terminally bound SO₂ can possess both coplanar and pyramidal MSO₂ geometry when binding to transition metals through the sulfur atom. Likewise, the O-bonded geometry has been observed in a complex of SO₂ with SbF₅.² However, the ability of SO₂ to bind to transition metals through both the sulfur atom and an oxygen atom simultaneously was not recognized prior to our preliminary communication of the structure of Rh(NO)(SO₂)(PPh₃)₂.¹ It

is interesting to note that this type of geometry does appear to be common for both CO₂ and CS₂ and has been structurally established in Ni(CO₂)(PCy₃)₂ (Cy = cyclohexyl)³ and Pt(CS₂)(PPh₃)₂.⁴ The extreme lability of the SO₂ in Rh(NO)(SO₂)(PPh₃)₂ had been observed previously and had hindered its isolation and characterization. Similarly its reaction with molecular oxygen to form a coordinated sulfate had been reported.⁵ The significance of these data, however, could only be recognized after the structural features of this

complex were elucidated, since these characteristics had previously been associated only with pyramidal MSO_2 complexes.

In this work we wish to report a further study into the nature of this novel coordination of sulfur dioxide by rhodium. The complete crystal structure analysis of $\text{Rh}(\text{NO})(\text{SO}_2)(\text{PPh}_3)_2$ is reported and an oxygen-18 labeling study of the sulfato reaction is examined.

Experimental Section

Reagents and Chemicals. All solvents used in this study were reagent grade and were used without purification. Sulfur dioxide was obtained from the Matheson Co. All $^{18}\text{O}_2$ was generated from oxygen-18 labeled nitric oxide, enriched at the Los Alamos Scientific Laboratory. $\text{Rh}(\text{NO})(\text{PPh}_3)_3$, $\text{Pt}(\text{SO}_2)_2(\text{PPh}_3)_2$, and $\text{RuCl}(\text{NO})(\text{PPh}_3)_2$ were prepared by literature procedures.⁶⁻⁸ Infrared spectra were run on Perkin-Elmer 521 and Perkin-Elmer 180 spectrometers (Nujol mulls).

Generation of $^{18}\text{O}_2$ from $^{15}\text{N}^{18}\text{O}$. A Pyrex vessel having approximately 600-mL volume and containing two metal electrodes separated by a 0.5-in. gap was filled with 200–300 Torr of labeled NO. A neon sign transformer was connected across the electrodes and the input voltage to the transformer increased until an arc was obtained. The gas turns dark brown initially from NO_2 generation and slowly clears as N_2 and O_2 are obtained. The conversion is more than 99% complete after 12 h and the residual NO_2 is separated by cooling a tip of the vessel with liquid N_2 . Aliquots of the gas are then expanded into previously evacuated reaction bulbs for subsequent use. Both 99 and 50% oxygen-18 labeled NO were used in the study. Isotopic purity of the resulting N_2 and O_2 mixture were monitored by mass spectral analysis. No attempt was made to separate the oxygen from the nitrogen in these mixtures.

$\text{Rh}(\text{NO})(\text{SO}_2)(\text{PPh}_3)_2 + \text{O}_2$. As a control experiment, 0.9 g (1 mmol) of $\text{Rh}(\text{NO})(\text{PPh}_3)_3$ was dissolved in 50 mL of benzene, saturated with SO_2 , and opened to a vessel containing 1 mmol of O_2 . During a period of 10 days, green crystals precipitated from the solution. The crystals were filtered, washed with heptane, and vacuum dried. Elemental analysis suggests the product to be pure $\text{Rh}(\text{NO})(\text{SO}_4)(\text{PPh}_3)_2$. Anal. Calcd for $\text{C}_{36}\text{H}_{30}\text{NP}_2\text{O}_4\text{SRh}$: C, 57.4; H, 4.00; N, 1.86; S, 4.26; P, 8.23. Found:⁹ C, 57.2; H, 4.01; N, 1.85; S, 4.39; P, 8.07. Infrared analysis of $\nu(\text{NO})$ and $\nu(\text{SO}_4)$ is consistent with that previously reported.⁵ The antisymmetric stretch of the two external oxygens of the sulfate (highest $\nu(\text{SO}_4)$) is observed at 1263 cm^{-1} ($^{16}\text{O}-^{16}\text{O}$).

A similar reaction was performed using 50% oxygen-18 labeled O_2 . Infrared analysis revealed three overlapping peaks in the region of the antisymmetric stretch, probably corresponding to $^{16}\text{O}-^{16}\text{O}$ (1263 cm^{-1}), $^{16}\text{O}-^{18}\text{O}$ (1248 cm^{-1}), and $^{18}\text{O}-^{18}\text{O}$ (1226 cm^{-1}). The magnitudes of these isotopic shifts are similar to that observed for other sulfato systems.¹⁰ Due to the overlapped nature of the peaks, an accurate intensity ratio could not be measured at room temperature; however, upon cooling to 14 K sufficient resolution was available that a ratio of 9:7:3 ($^{16}\text{O}-^{16}\text{O}$: $^{16}\text{O}-^{18}\text{O}$: $^{18}\text{O}-^{18}\text{O}$) could be measured with limited accuracy. Similarly, when 99.7% oxygen-18 O_2 was reacted with $\text{Rh}(\text{NO})(\text{SO}_2)(\text{PPh}_3)_2$ as above, a ratio of 1:2:1 for these peaks was observed.

$\text{RuCl}(\text{NO})(\text{SO}_2)(\text{PPh}_3)_2 + ^{18}\text{O}_2$. $\text{RuCl}(\text{NO})(\text{PPh}_3)_2$ was prepared in benzene solution and reacted with excess gaseous SO_2 to form $\text{RuCl}(\text{NO})(\text{SO}_2)(\text{PPh}_3)_2$.¹¹ Addition of heptane precipitated the red-orange solid with an infrared spectrum containing $\nu(\text{SO}_2)$ at $1330-1311\text{ cm}^{-1}$ (asym) and $1140-1130\text{ cm}^{-1}$ (sym) and $\nu(\text{NO})$ at 1770 cm^{-1} .

Similarly, 0.25 mmol of $\text{RuCl}(\text{NO})(\text{SO}_2)(\text{PPh}_3)_2$ was prepared in 50 mL of SO_2 -saturated benzene. This solution was allowed to react with 0.5 mmol of O_2 (98% oxygen-18) for 5 days. The orange crystals of $\text{RuCl}(\text{NO})(\text{SO}_4)(\text{PPh}_3)_2$ thus formed were filtered, washed with heptane, and vacuum dried. The antisymmetric stretch of the two terminal oxygens of the coordinated sulfate was observed at 1278 cm^{-1} , in the region expected for $^{16}\text{O}-^{18}\text{O}$ isotopic content. A small peak, barely observable above the noise, was present at 1294 cm^{-1} ($^{16}\text{O}-^{16}\text{O}$; lit. 1300 cm^{-1}).^{10,12} No appreciable $^{18}\text{O}-^{18}\text{O}$ peak could be observed in the predicted region between 1260 and 1250 cm^{-1} .

$\text{Pt}(\text{SO}_2)_2(\text{PPh}_3)_2 + ^{18}\text{O}_2$. A benzene solution containing 0.2 mmol of $\text{Pt}(\text{SO}_2)_2(\text{PPh}_3)_2$ was reacted with a threefold excess of O_2 (98% oxygen-18) for 5 days. The solution was then evaporated to dryness, leaving the off-white $\text{Pt}(\text{SO}_4)(\text{PPh}_3)_2$ in the vessel. An infrared

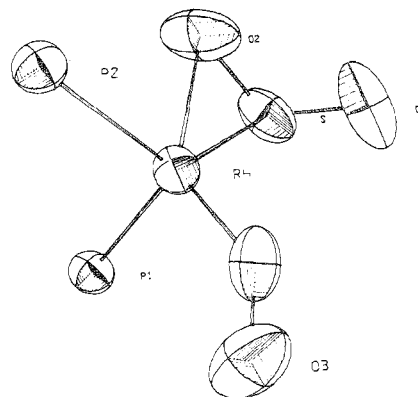


Figure 1. Coordination around rhodium with thermal ellipsoids drawn at the 50% probability level.

spectrum of the region involving the antisymmetric stretch of the terminal oxygens of the sulfato group contained only one peak, corresponding to $^{16}\text{O}-^{18}\text{O}$ isotopic content and falling at 1262 cm^{-1} . As previously reported,¹⁰ the peaks in this region are broad and poorly resolved for this complex; however, sufficient resolution was obtained such that the presence of $^{16}\text{O}-^{16}\text{O}$ or $^{18}\text{O}-^{18}\text{O}$ peaks of more than 15–20% abundance would have been detectable.

Crystal Structure Analysis. Crystals of $\text{Rh}(\text{NO})(\text{SO}_2)(\text{PPh}_3)_2$ were prepared as previously reported¹ and coated with mineral oil to slow decomposition in the air.

Precession photographs revealed diffraction patterns consistent with the space group $Pbca$. An elongated wedge-shaped crystal of approximate dimensions $0.45 \times 0.19 \times 0.11\text{ mm}$ was mounted along the long direction of the crystal and placed on a Picker FACS-I diffractometer. The cell constants obtained from least-squares refinement of 12 high-order reflections are $a = 10.338(2)\text{ \AA}$, $b = 18.500(4)\text{ \AA}$, $c = 33.933(7)\text{ \AA}$, $d_c = 1.48\text{ g cm}^{-3}$, $d_m = 1.47\text{ g cm}^{-3}$, and $Z = 8$ ($\text{Cu K}\alpha_1$ radiation, $\lambda = 1.54051\text{ \AA}$).

Intensities were measured using $\text{Cu K}\alpha$ radiation filtered by a 1-mil thickness of Ni foil. A standard $\theta-2\theta$ scan technique, 1.5° (plus $\alpha_1-\alpha_2$ dispersion) scan at $2^\circ/\text{min}$ and 20 s background at each extreme of the scan, was utilized to collect 3601 reflections ($2 \leq 2\theta \leq 100^\circ$). Of the 3145 unique reflections obtained after averaging equivalent reflections, 2615 were observed with $I > 2\sigma(I)$ (where $\sigma(I)$ was computed as usual)¹³ and were used in the solution and refinement of the structure. The intensities of two standard reflections measured every 50 reflections indicated a drop in intensity of approximately 10% during the data collection. Recentering the initial 12 high-order reflections and least-squares refinement failed to restore the initial intensity to the standards, as this decay of the standards was due to slight crystal decomposition and not misalignment. These fluctuations in the data were corrected using a polynomial determined by least-squares fitting the standard reflection curves. Absorption corrections were applied¹⁴ ($\mu = 61.62\text{ cm}^{-1}$) assuming a crystal bounded by five faces $\{100\}$, $\{094\}$, $\{0,-9,4\}$, and $\{0,0,-1\}$. The transmission factors varied between 0.73 and 0.43.

The rhodium atom was located using standard Patterson techniques and all nonhydrogen atoms were located using difference Fourier techniques. Although the majority of the hydrogen atoms were visible in the difference Fourier maps, these were not refined but were placed in idealized positions¹⁵ and given isotropic thermal parameters of 5.0. Refinement was performed as described in previous publications¹³ using neutral atom scattering factors¹⁶ and appropriate dispersion terms.¹⁷ All atoms, other than hydrogen, were refined anisotropically. The final refinement including a secondary extinction correction^{18,19} yielded an unweighted R value of 0.038. Final atomic parameters are given in Table I with anisotropic thermal parameters listed in Table II and pertinent distances and angles are given in Table III.

Results and Discussion

Molecular Structure. A picture of the rhodium coordination is shown in Figure 1 and a stereoview of the structure is shown in Figure 2. Examination of these figures and the distances and angles listed in Table III clearly establishes that the SO_2 is S,O-bonded to rhodium. As is the case with other small molecules which are capable of attachment to a metal atom

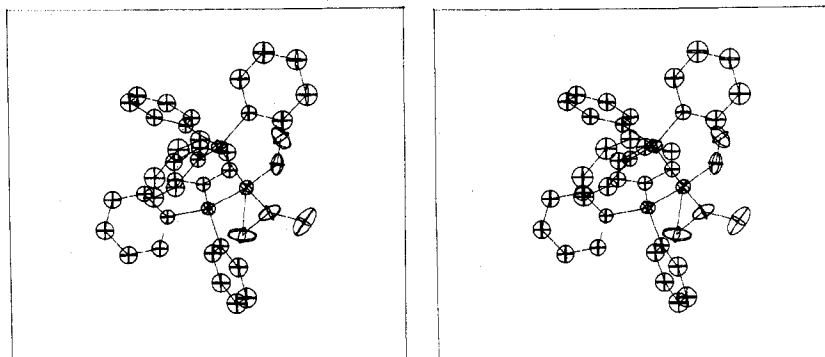


Figure 2. A stereoview of the molecular structure.

Table I. Atomic Coordinates^a

Atom	x	y	z
Rh	0.02526 (5)	0.05109 (3)	0.13155 (1)
S	-0.0714 (2)	0.0104 (1)	0.18935 (5)
O1	-0.1076 (6)	-0.0631 (3)	0.1825 (2)
O2	-0.1584 (5)	0.0655 (3)	0.1712 (1)
N	0.1174 (7)	-0.0196 (3)	0.1082 (2)
O3	0.2230 (6)	-0.0308 (3)	0.0952 (2)
P1	0.1819 (2)	0.11100 (9)	0.16624 (5)
P2	-0.0604 (2)	0.12923 (9)	0.08129 (5)
C1	0.2686 (6)	0.1804 (3)	0.1393 (2)
C2	0.2996 (6)	0.2475 (4)	0.1547 (2)
C3	0.3610 (7)	0.2992 (4)	0.1325 (2)
C4	0.3960 (8)	0.2842 (4)	0.0940 (2)
C5	0.3693 (7)	0.2186 (4)	0.0784 (2)
C6	0.3051 (6)	0.1653 (4)	0.1005 (2)
C7	0.3085 (7)	0.0500 (4)	0.1832 (2)
C8	0.4376 (8)	0.0675 (4)	0.1817 (2)
C9	0.5291 (8)	0.0195 (5)	0.1959 (3)
C10	0.4966 (9)	-0.0448 (5)	0.2113 (2)
C11	0.3668 (10)	-0.0634 (4)	0.2129 (2)
C12	0.2759 (7)	-0.0164 (4)	0.1987 (2)
C13	0.1312 (7)	0.1594 (3)	0.2103 (2)
C14	0.0267 (7)	0.2061 (4)	0.2077 (2)
C15	-0.0075 (7)	0.2502 (4)	0.2385 (2)
C16	0.0631 (8)	0.2476 (5)	0.2727 (2)
C17	0.1629 (8)	0.2005 (5)	0.2765 (2)
C18	0.2000 (7)	0.1567 (4)	0.2455 (2)
C19	-0.0922 (7)	0.2213 (3)	0.0984 (2)
C20	0.0033 (7)	0.2723 (4)	0.1019 (2)
C21	-0.0196 (8)	0.3396 (4)	0.1185 (2)
C22	-0.1424 (9)	0.3562 (4)	0.1327 (2)
C23	-0.2391 (7)	0.3055 (4)	0.1295 (2)
C24	-0.2160 (7)	0.2384 (4)	0.1131 (2)
C25	0.0405 (7)	0.1379 (4)	0.0370 (2)
C26	0.0987 (7)	0.0756 (4)	0.0233 (2)
C27	0.1757 (8)	0.0773 (4)	-0.0098 (2)
C28	0.1968 (8)	0.1404 (4)	-0.0294 (2)
C29	0.1375 (8)	0.2027 (4)	-0.0171 (2)
C30	0.0578 (7)	0.2019 (3)	0.0161 (2)
C31	-0.2185 (7)	0.1002 (4)	0.0616 (2)
C32	-0.3024 (8)	0.0636 (4)	0.0853 (2)
C33	-0.4270 (7)	0.0454 (5)	0.0720 (3)
C34	-0.4609 (9)	0.0634 (5)	0.0337 (3)
C35	-0.3768 (10)	0.0979 (4)	0.0091 (2)
C36	-0.2528 (8)	0.1167 (4)	0.0223 (2)

^a With a secondary extinction correction of $2.2 (5) \times 10^{-5}$ and a scale factor of 0.5567 (9).

to form a three-membered ring, i.e., O₂, CS₂, CO₂, and C₂H₄, the SO bond distance in the ring (1.493 Å) is significantly longer than that found when the perturbing effect of the metal atom is not present. An average S–O distance for S-bonded SO₂ is approximately 1.45 Å and the S–O(1) distance of 1.430 Å and the O–S–O angle of 115.1 (4)° are within the range established by previous investigations. This latter observation is interesting in relation to the structural information available for side-bonded CS₂ and CO₂ in (PPh₃)₂PtCS₂⁴ and (Cy₃P)₂NiCO₂³ in which the large deviations of the ligand

molecules from linearity have been attributed to excited-state electronic configurations. In the present case we note that the parameters for SO₂ are closer to the ground-state²⁰ values of $r = 1.432 (1)$, $\angle = 119.54^\circ$ for the free molecule, than the spectroscopically established values of $r = 1.494$, $\angle = 123.10^\circ$ for the ³B₁ state,²¹ as is, indeed, the case for all S-bound M–SO₂ complexes whose structures have been determined.

Within the framework of previously proposed bonding models^{22,23} and on the basis of previous structural work, one might have predicted a complex of this stoichiometry to contain tetrahedrally coordinated rhodium with a linear nitrosyl and a sulfur-bound sulfur dioxide exhibiting pyramidal geometry at the sulfur atom. A complex of this general description with a coplanar Rh–SO₂ group would not have been too surprising since it has been suggested that the presence of good π -acceptor ligands, such as nitrosyl, might favor the coplanar geometry. Since we feel that inspection of distance and angles reveals no palatable description of this complex in terms of a five-coordinate geometry and, in particular, since the angles around rhodium not involving the SO₂ ligand appear to favor a tetrahedral description for the metal coordination with \angle N–Rh–P1 = 101.8 (2)°, \angle N–Rh–P2 = 108.7 (2)°, and \angle P1–Rh–P2 = 109.37 (6)°, we choose to discuss the geometry of this complex from the latter point of view. This viewpoint makes the M–N–O angle 140.4 (6)° observed here particularly interesting. The only other complex of this type in which the MNO deviates significantly from linearity is Ni(N₃)(NO)-(PPh₃)₂²² in which the angle is 153°. This bending of the nitrosyl in the Ni complex has been correlated with a distortion toward square-planar geometry; however, no such distortion is observed in the structure of Rh(NO)(SO₂)(PPh₃)₂.

We notice that this complex has some features which are reminiscent of previously studied transition-metal complexes containing two amphoteric ligands;²⁴ i.e., the nitrosyl ligand is bent away from the SO₂ and toward P2, the angle between the N–O vector and the P2–Rh–N plane being approximately 20°, while the S–O2 vector lies approximately in the P2–Rh–S plane. In a generalized sense this behavior has been observed in (PPh₃)₂Pt(SO₂)₂ as well as in many of the bis(nitrosyl) complexes. In the latter type of system a N–N interaction has been postulated to account for their catalytic behavior²⁵ toward CO to form CO₂ and N₂O. We feel that a similar interligand interaction may provide a reasonable rationalization for the unusual geometries of the two amphoteric ligands under discussion here.

A rather tenuous suggestion can be made for the nature of the interaction by consideration of a hypothetical starting model in which the M–SO₂ group is planar, with the nitrosyl group attached to the metal in this plane. As previously pointed out, there apparently exists very little interaction between the metal d orbitals and the orbitals in the SO₂ plane for this geometry. Orbital participation in this plane could be promoted by the raising of the d-orbital energy due to π interaction with the nitrosyl. Within the framework of our

Table II. Anisotropic Thermal Parameters ($\times 10^4$)

Atom	β_{11}	β_{22}	β_{33}	$2\beta_{12}$	$2\beta_{13}$	$2\beta_{23}$
Rh	75.3 (7)	22.5 (2)	6.19 (5)	-7.7 (6)	-3.8 (3)	-1.4 (2)
S	103 (3)	46.1 (9)	7.7 (2)	-44 (3)	3 (1)	5.5 (7)
O1	242 (10)	50 (2)	16.1 (7)	-130 (9)	19 (4)	-2 (2)
O2	83 (7)	80 (3)	12.5 (6)	16 (8)	24 (3)	13 (2)
N	148 (10)	24 (2)	8.4 (7)	-12 (8)	-5 (4)	-2 (2)
O3	171 (10)	48 (3)	14.4 (7)	57 (8)	19 (4)	-2 (2)
P1	70 (2)	24.6 (6)	6.4 (2)	-5 (2)	0 (1)	1.3 (6)
P2	77 (2)	23.6 (6)	6.1 (2)	3 (2)	-5 (1)	-0.6 (5)
C1	53 (8)	26 (3)	6.2 (7)	17 (8)	-3 (4)	3 (2)
C2	82 (10)	28 (3)	7.8 (7)	-8 (9)	2 (4)	-1 (3)
C3	119 (11)	25 (3)	12.0 (9)	-27 (9)	-2 (6)	3 (3)
C4	107 (11)	33 (3)	12 (1)	-12 (10)	17 (6)	9 (3)
C5	101 (11)	41 (3)	8.8 (8)	16 (10)	21 (5)	3 (3)
C6	67 (9)	30 (3)	9.3 (8)	4 (8)	9 (4)	1 (3)
C7	77 (10)	22 (2)	6.6 (7)	7 (8)	-1 (4)	4 (2)
C8	82 (11)	35 (3)	12.5 (9)	-2 (10)	2 (5)	8 (3)
C9	68 (10)	49 (4)	14 (1)	34 (11)	4 (5)	1 (3)
C10	117 (13)	40 (3)	9.8 (8)	50 (11)	-9 (5)	1 (3)
C11	151 (14)	31 (3)	14 (1)	-5 (11)	-20 (6)	12 (3)
C12	85 (11)	35 (3)	13.5 (9)	5 (10)	-13 (5)	11 (3)
C13	68 (9)	25 (2)	6.1 (7)	-11 (8)	6 (4)	1 (2)
C14	105 (10)	30 (3)	8.4 (8)	13 (10)	1 (5)	-3 (2)
C15	90 (11)	31 (3)	14 (1)	7 (9)	16 (6)	-6 (3)
C16	113 (13)	52 (4)	9 (1)	-25 (12)	21 (6)	-16 (3)
C17	99 (12)	64 (4)	8.5 (9)	-1 (12)	-2 (5)	-13 (3)
C18	84 (10)	39 (3)	8.4 (8)	19 (9)	-1 (5)	-1 (3)
C19	76 (9)	24 (2)	4.8 (6)	12 (9)	0 (4)	0 (2)
C20	96 (10)	26 (3)	7.5 (7)	-2 (9)	-9 (4)	-4 (2)
C21	113 (12)	26 (3)	10.1 (8)	-9 (9)	-17 (5)	-5 (2)
C22	138 (12)	32 (3)	7.7 (8)	38 (11)	-16 (5)	-10 (3)
C23	100 (10)	36 (3)	7.4 (7)	16 (9)	1 (5)	-4 (3)
C24	117 (11)	23 (3)	6.6 (7)	-6 (9)	0 (5)	-1 (2)
C25	91 (9)	26 (2)	5.1 (6)	2 (8)	-9 (4)	0 (2)
C26	126 (11)	26 (3)	6.2 (7)	14 (9)	-6 (5)	1 (2)
C27	162 (13)	34 (3)	7.7 (8)	49 (10)	16 (5)	-2 (3)
C28	128 (12)	41 (3)	7.7 (8)	17 (11)	12 (5)	0 (3)
C29	163 (13)	34 (3)	7.1 (8)	-19 (11)	13 (5)	4 (3)
C30	121 (11)	25 (3)	7.6 (7)	18 (9)	-4 (5)	1 (2)
C31	92 (11)	27 (3)	8.1 (8)	19 (9)	-22 (5)	-10 (2)
C32	126 (13)	37 (3)	11.4 (9)	-32 (10)	22 (6)	-1 (3)
C33	63 (11)	52 (4)	21 (1)	-36 (11)	-20 (6)	-38 (4)
C34	133 (14)	49 (4)	15 (1)	31 (12)	-45 (7)	-27 (4)
C35	144 (15)	36 (3)	14 (1)	17 (11)	-28 (7)	-4 (3)
C36	98 (11)	30 (3)	15 (1)	7 (9)	-43 (6)	-9 (3)

Table III. Distances and Angles

Distances, Å			
Rh-S	2.326 (2)	N-O3	1.195 (7)
Rh-O2	2.342 (5)	P1-C1	1.813 (6)
Rh-N	1.802 (6)	P1-C7	1.821 (6)
Rh-P1	2.288 (2)	P1-C13	1.819 (6)
Rh-P2	2.410 (2)	P2-C19	1.820 (6)
S-O1	1.430 (5)	P2-C25	1.836 (6)
S-O2	1.493 (5)	P2-C31	1.848 (7)
Angles, Deg			
S-Rh-O2	37.3 (1)	Rh-N-O3	140.4 (6)
S-Rh-N	111.3 (2)	Rh-P1-C1	115.7 (2)
S-Rh-P1	91.53 (6)	Rh-P1-C7	111.8 (2)
S-Rh-P2	129.36 (7)	Rh-P1-C13	117.2 (2)
O2-Rh-N	139.8 (2)	C1-P1-C7	104.1 (3)
O2-Rh-P1	102.9 (1)	C1-P1-C13	102.0 (3)
O2-Rh-P2	92.3 (1)	C7-P1-C13	104.6 (3)
N-Rh-P1	101.8 (2)	Rh-P2-C19	113.8 (2)
N-Rh-P2	108.7 (2)	Rh-P2-C25	114.9 (2)
P1-Rh-P2	109.37 (6)	Rh-P2-C31	113.7 (2)
Rh-S-O1	106.4 (2)	C19-P2-C25	106.6 (3)
Rh-S-O2	71.9 (2)	C19-P2-C31	103.3 (3)
O1-S-O2	115.1 (4)	C25-P2-C31	103.3 (3)
Rh-O2-S	70.8 (2)		

previous discussions, the resulting orbital obviously has the proper symmetry to couple with the in-plane wagging motion of the SO_2 and promote bending in this plane. The resulting side-on bond SO_2 apparently exhibits better donor properties

than does the S-bonded ligand, thereby contributing to the bending of the nitrosyl group. Although the exact nature of this ligand-ligand interaction defies a simple explanation, we are hopeful that theoretical studies now under way will provide additional insight into this problem as will the characterization of similar isoelectronic systems. We finally point out the $\text{O}_2\text{-S-N}$ angle of 97° is near enough to the tetrahedral angle so that it may also be indicative of a ligand-ligand interaction.

The reaction of transition-metal oxygen complexes with SO_2 has been studied by collman and co-workers using oxygen-18 labeling and infrared spectroscopy.¹⁰ The highest frequency peak of the coordinated sulfate, involving the antisymmetric stretch of the two external oxygens, was used as a diagnostic to probe the distribution of the label in the products. Based on the relative intensities of the stretches involving the three isotopic species ($^{16}\text{O}\text{-}^{16}\text{O}$, $^{16}\text{O}\text{-}^{18}\text{O}$, $^{18}\text{O}\text{-}^{18}\text{O}$), a peroxy-sulfite-type intermediate was proposed. This type of intermediate was invoked to account for the experimental observation that one of the two external oxygens of the bidentate sulfate group comes from the M-O_2 molecular unit while the other comes from the SO_2 molecule. The structural similarities of this proposed intermediate to the S,O-bonded SO_2 geometry observed in $\text{Rh}(\text{NO})(\text{SO}_2)(\text{PPh}_3)_2$ suggested that further labeling studies were warranted.

Utilizing similar techniques to those reported by Collman and co-workers,¹⁰ we have studied the sulfato reactions of both S- and S,O-bonded SO_2 . In the former category both

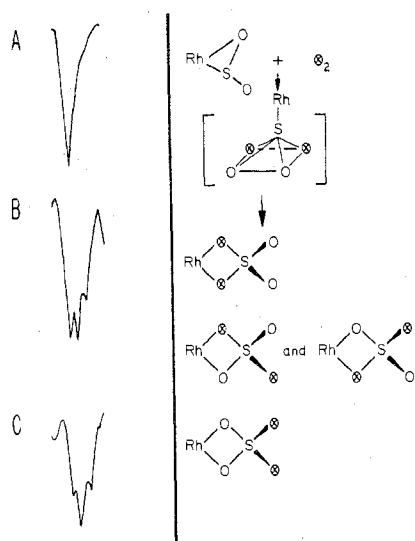


Figure 3. Distribution of the oxygen-18 label in the reaction of Rh(NO)(SO₂)(PPh₃)₂ with ¹⁸O₂. Infrared spectral analysis utilizing: (A) normal isotopic content O₂, (B) 50% oxygen-18 substitution, (C) 99.7% ¹⁸O₂.

RuCl(NO)(SO₂)(PPh₃)₂ and Pt(SO₂)₂(PPh₃)₂ were studied. These were chosen for three reasons: (1) the crystal structures of both sulfato products have been determined and found to possess the bidentate sulfato coordination;^{12,26} (2) the anti-symmetric stretches of the two terminal oxygens (ν_{3a}) of the sulfato groups for these two complexes fall in regions of little interference from overlapping bands; (3) the S-bonded geometry has been established by an x-ray crystal structure determination in Pt(SO₂)₂(PPh₃)₂ and can be inferred from the infrared spectrum of RuCl(NO)(SO₂)(PPh₃)₂.

Examination of the infrared spectrum of RuCl(NO)(SO₄)(PPh₃)₂, formed by reaction of RuCl(NO)(SO₂)(PPh₃)₂ with 98% ¹⁸O₂, reveals a sharp peak in the region of ν_{3a} . The shift of 16 cm⁻¹ to lower frequency is in accord with the isotopic species ¹⁶O¹⁸O. Though a very small ¹⁶O¹⁶O peak was visible, no ¹⁸O¹⁸O component could be measured. These data suggest that one of the terminal oxygens of the sulfate group came from the ¹⁸O₂ while the other came from Ru-SO₂. This is the same situation observed in the reaction of M-O₂ with SO₂ and suggests a peroxysulfite-type intermediate. The reaction of Pt(SO₂)₂(PPh₃)₂ with 98% ¹⁸O₂ to form Pt(SO₄)(PPh₃)₂ proved to be a little more difficult to interpret because of the broadness of ν_{3a} . However, the peak maximum occurred at 1262 cm⁻¹ in the region of ¹⁶O¹⁸O. Although some contribution of ¹⁶O¹⁶O and ¹⁸O¹⁸O could be present under the broad peak, sufficient resolution was available that a distribution of 1(¹⁶O¹⁶O):2(¹⁶O¹⁸O):1(¹⁸O¹⁸O) could be excluded. Although more ambiguous than the ruthenium system, this also suggests a peroxysulfite intermediate.

The reaction of the S,O-bonded SO₂ in Rh(NO)(SO₂)(PPh₃)₂ with molecular O₂ was studied and the results are depicted in Figure 3. Reaction with a stoichiometric amount of O₂ (normal isotopic content) resulted in the formation of pure crystalline Rh(NO)(SO₄)(PPh₃)₂ with the ν_{3a} (¹⁶O¹⁶O) shown in Figure 3A, occurring at 1263 cm⁻¹ (lit. 1265 cm⁻¹).⁵ A single-crystal x-ray diffraction study of this material has confirmed the bidentate nature of the sulfate group²⁷ and the expected square-pyramidal geometry with a bent nitrosyl in the axial position. Upon reaction of Rh(NO)(SO₂)(PPh₃)₂ with 50% oxygen-18 labeled O₂, the ν_{3a} region of the infrared spectrum contained three peaks at 1263, 1248, and 1226 cm⁻¹ (Figure 3B). These peaks correspond to ¹⁶O¹⁶O, ¹⁶O¹⁸O, and ¹⁸O¹⁸O isotopic content in the terminal oxygen of the sulfato group, respectively. Accurate integration of the peaks was

hindered by overlap but the existence of the ¹⁸O¹⁸O peak suggested a different mechanism from that observed in the previous systems. Reaction with 99.7% ¹⁸O₂ resulted in the spectrum shown in Figure 3C. The same three peaks in the ν_{3a} region were observed but the intensity distribution here was clearly 1:2:1. These data support the mechanism depicted on the right side of Figure 3.

The central theme of this proposed mechanism involves the attack of oxygen on the sulfur atom and the formation of an intermediate containing square-pyramidal sulfur coordination. The oxygen atoms become equivalent in the basal plane, allowing the apical metal to move to each of the four basal edges with equal probability. The isotopic distribution in the resulting bidentate sulfate group is pictured in Figure 3. Clearly, for the 99.7% ¹⁸O₂ experiment, one would predict a 1:2:1 ratio in the sulfato product. The intensity ratio of 9:7:3 observed in the 50% ¹⁸O labeling study also compares favorably with the calculated ratio of 9:6:1 which is derived from the model pictured. Although the square-pyramidal sulfur coordination of the proposed intermediate might seem chemically unreasonable, it should be noted that we have been unable to propose another intermediate containing better documented sulfur coordination which appears to satisfy the data. It should also be noted that simple metal tautomerism about the sulfato group can be discounted as this would lead to a 1:4:1 intensity pattern in the 99.7% ¹⁸O₂ experiment.

Although the data presented here indicate that the mechanism for the sulfato reaction in this complex is different from that proposed for the MO₂ and S-bonded MSO₂ systems, we believe that there exists a ready explanation for this difference. That is to say that we feel that the (SO₂-NO) interligand interaction is similar to the interaction which takes place between SO₂ and O₂ in the previously studied systems, the function of which is to promote the affinity of the bound sulfur atom for further attack by the metal-bound O₂ resulting in Collman's proposed intermediate. If this hypothesis is true, then it is not unreasonable to suppose that since this function is already provided by the nitrosyl here, the result is direct attack on the sulfur atom by molecular oxygen leading to a different reaction pathway to the sulfato complex.

In conclusion, it appears that the factors influencing the S,O bonding of SO₂ as well as the nature of the ligand itself will remain uncertain until more examples of this type are discovered. Similarly, its role in the sulfato reaction mechanism will probably remain in doubt until more reactions of this type can be studied.

Acknowledgment. This work was performed under the auspices of the U.S. Energy Research and Development Administration.

Registry No. Rh(NO)(SO₂)(PPh₃)₂, 60633-55-8; Rh(NO)(SO₄)(PPh₃)₂, 62249-56-3; RuCl(NO)(SO₂)(PPh₃)₂, 63743-81-7; RuCl(NO)(SO₄)(PPh₃)₂, 52760-71-1; Pt(SO₂)₂(PPh₃)₂, 59187-63-2; Pt(SO₄)(PPh₃)₂, 12577-89-8; O₂, 7782-44-7; ¹⁸O₂, 32767-18-3.

Supplementary Material Available: Listing of structure factor amplitudes (13 pages). Ordering information is given on any current masthead page.

References and Notes

- (1) A preliminary communication of this crystal structure has appeared: D. C. Moody and R. R. Ryan, *J. Chem. Soc., Chem. Commun.*, 503 (1976).
- (2) J. W. More, H. W. Baird, and H. B. Miller, *J. Am. Chem. Soc.*, **90**, 1358 (1968).
- (3) M. Aresta, C. F. Nobile, V. G. Albano, E. Forni, and M. Manassero, *J. Chem. Soc., Chem. Commun.*, 636 (1975).
- (4) R. Mason and A. I. M. Rae, *J. Chem. Soc. A*, 1767 (1970).
- (5) J. Valentine, D. Valentine, Jr., and J. P. Collman, *Inorg. Chem.*, **10**, 219 (1971).
- (6) N. Ahmod, J. J. Levison, S. D. Robinson, and M. F. Uttley, *Inorg. Synth.*, **15**, 61 (1974).
- (7) C. D. Cook and G. S. Jauhal, *J. Am. Chem. Soc.*, **89**, 3066 (1967).
- (8) J. Reed, C. G. Pierpont, and R. Eisenberg, *Inorg. Synth.*, **16**, 21 (1975).

- (9) Analyses performed by Galbraith Laboratories, Inc., Knoxville, Tenn.
 (10) R. W. Horn, E. Weissburger, and J. P. Collman, *Inorg. Chem.*, **9**, 2367 (1970).
 (11) M. H. B. Stiddard and R. E. Townsend, *Chem. Commun.*, 1372 (1969).
 (12) J. Reed, S. L. Soled, and R. Eisenberg, *Inorg. Chem.*, **13**, 3001 (1974).
 (13) R. R. Ryan and B. I. Swanson, *Inorg. Chem.*, **13**, 1681 (1974).
 (14) P. Coppens, J. de Meulenaer, and H. Tompa, *Acta Crystallogr.*, **22**, 601 (1967), using a recent modification of Dr. L. Templeton (private communication).
 (15) M. R. Churchill, *Inorg. Chem.*, **12**, 1213 (1973).
 (16) D. T. Cromer, "International Tables for X-Ray Crystallography", Kynoch Press, Birmingham, England, in press.
 (17) D. T. Cromer and D. Liberman, *J. Chem. Phys.*, **53**, 1891 (1970).
 (18) W. J. Zachariasen, *Acta Crystallogr.*, **23**, 558 (1967).
 (19) A. C. Larson, *Acta Crystallogr.*, **23**, 664 (1967).
 (20) D. Kivetsen, *J. Chem. Phys.*, **22**, 904 (1954).
 (21) A. J. Merer, *Discuss. Faraday Soc.*, **35**, 127 (1963).
 (22) J. H. Enemark and R. D. Feltham, *Coord. Chem. Rev.*, **13**, 339 (1974).
 (23) R. R. Ryan and P. G. Eller, *Inorg. Chem.*, **15**, 494 (1976).
 (24) B. L. Haymore and J. A. Ibers, *Inorg. Chem.*, **14**, 2610 (1975).
 (25) B. L. Haymore and J. A. Ibers, *J. Am. Chem. Soc.*, **96**, 3325 (1974).
 (26) C. G. Pierpont, *ACA Newsletter*, **6**, 12 (1975); private communication.
 (27) B. C. Lucas, D. C. Moody, and R. R. Ryan, *Cryst. Struct. Commun.*, **6**, 57 (1977).

Contribution from the Department of Inorganic Chemistry,
 University of Sydney, Sydney, New South Wales 2006, Australia

Stabilization of High Oxidation States by Strong Electron-Donating Ligands. Crystal Structure and Properties of Tetra-*n*-butylammonium *o*-Phenylenebis(biuretato)cuprate(III)-Chloroform, $(n\text{-C}_4\text{H}_9)_4\text{NCu}[o\text{-C}_6\text{H}_4(\text{NCONHCONH})_2]\cdot\text{CHCl}_3$

PAUL J. M. W. L. BIRKER

Received March 18, 1977

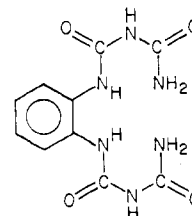
AIC702112

The Cu^{III} complex of *o*-phenylenebis(biuret) can be obtained by oxidation of the parent Cu^{II} complex with iodine. Tetra-*n*-butylammonium *o*-phenylenebis(biuretato)cuprate(III)-chloroform, $(n\text{-C}_4\text{H}_9)_4\text{NCu}[o\text{-C}_6\text{H}_4(\text{NCONHCONH})_2]\cdot\text{CHCl}_3$, crystallizes with a triclinic unit cell, $a = 9.68$ (1) Å, $b = 10.75$ (1) Å, $c = 16.64$ (4) Å, $\alpha = 93.4$ (1)°, $\beta = 105.2$ (1)°, $\gamma = 94.32$ (5)°, and $V = 1660$ (8) Å³; $d_{\text{measd}} = 1.44$ g cm⁻³ and $d_{\text{calcd}} = 1.403$ g cm⁻³ for $Z = 2$. The structure was solved by standard Patterson and Fourier methods and refined by full-matrix least squares to a residual of 0.079 for 3075 independent reflections whose intensities were measured on an automatic diffractometer. The Cu atom is planar coordinated by four deprotonated amide nitrogen atoms. The $\text{Cu}^{\text{III}}\text{-N}$ bond lengths (1.82–1.89 Å) are shorter than the $\text{Cu}^{\text{II}}\text{-N}$ distances in related Cu^{II} complexes and comparable with $\text{Ni}^{\text{II}}\text{-N}$ (peptide) bond lengths. This is an indication that Cu^{III} (d^8) is the correct description for the oxidation state of the metal. The unusual redox behavior, coordination geometry, magnetic properties, and reactivity of Co, Ni, or Cu complexes with biuret or peptides can be understood on the basis of strong electron donation by the deprotonated amide groups and redox processes at the metal center. Electrochemical and NMR data for the complex are reported.

Introduction

In previous publications¹⁻³ the synthesis and physical properties of complexes of trivalent Cu, Ni, or Co with ligands coordinating via deprotonated amide groups were reported. Stable bis(bidentate)-chelated Cu^{III} complexes were prepared with biuret ($\text{H}_2\text{N-CO-NH-CO-NH}_2$, biH_2),⁴ 3-propylbiuret ($\text{H}_2\text{N-CO-N}(\text{C}_3\text{H}_7)\text{-CO-NH}_2$), and oxamide ($\text{H}_2\text{N-CO-CO-NH}_2$). Only the complexes with alkyl-substituted biuret are soluble (e.g., in dimethyl sulfoxide, acetone, and ethanol). Spectroscopic, magnetic, and polarographic data were shown to be consistent with planar bis(bidentate) chelation of the Cu atom by two $(\text{HN-CO-NR-CO-NH})^{2-}$ ligands ($\text{R} = \text{H}$ or $-\text{C}_3\text{H}_7$).² The crystal structure analysis of the parent Cu^{II} complex $\text{K}_2\text{Cu}(\text{bi})_2\cdot 4\text{H}_2\text{O}$ had previously revealed this type of metal coordination.⁵ It has also been found in paramagnetic Co^{III} complexes with 3-phenylbiuret⁶ and 3-*n*-propylbiuret⁷ [$(\text{HN-CO-NR-CO-NH})^{2-}$ with $\text{R} = \text{C}_6\text{H}_5$ and $n\text{-C}_3\text{H}_7$, respectively]. Crystals of a Cu^{III} -biuret complex suitable for x-ray diffraction could previously not be obtained.

Metal binding via deprotonated amide groups also occurs in complexes with amino acid amide and peptide ligands, and these species may be oxidized to the corresponding Cu^{III} complexes.⁸⁻¹¹ However, no crystalline derivatives of copper(III) peptide complexes have so far been prepared, probably because these compounds are relatively unstable. A half-life of only 2 h has been reported for a solution of a copper(III) triglycylglycinato complex at 25 °C and optimum pH conditions.¹¹ Intramolecular ligand oxidation is followed by fragmentation of the peptide.^{8,9} Recently crystals were obtained of a new Cu^{III} complex with *o*-phenylenebis(biuret) [$o\text{-C}_6\text{H}_4(\text{NH-CO-NH-CO-NH}_2)_2$, *o*-phen(bi)₂H₄]. We now



report its x-ray crystal structure and discuss some of the properties of Co, Ni, and Cu complexes with this type of ligand.

Experimental Section

o-Phenylenebis(biuret) was prepared according to the previously published method³ with slight modifications which were found to improve the yield. *o*-Phenylenediamine (BDH, reagent grade) was recrystallized from toluene. Nitrobiuret ($\text{H}_2\text{N-CO-NH-CO-NH-NO}_2$) was freshly prepared.¹² Nitrobiuret (3 g, 0.02 mol) and *o*-phenylenediamine (1.1 g, 0.01 mol) were suspended in water (35 mL). The mixture was flushed with nitrogen and stirred under nitrogen on a water bath at 70 °C for 2 h. The reagents slowly dissolved and from the clear solution *o*-phenylenebis(biuret) precipitated spontaneously or precipitated on heating the solution to 100 °C. Finally the mixture was kept at 100 °C for 15 min and the product was obtained from the hot solution by filtration and washed with cold water.

$(n\text{-C}_4\text{H}_9)_4\text{NCu}^{\text{III}}[o\text{-phen}(\text{bi})_2]\cdot\text{CHCl}_3$, $\text{CuCl}_2\cdot 2\text{H}_2\text{O}$ (0.34 g, 2 mmol), *o*-phenylenebis(biuret) (0.56 g, 2 mmol) and I_2 (0.35 g, 0.7 mmol) were dissolved in a mixture of Me_2SO (20 mL) and water (5 mL). To this solution 5 mL of a $(n\text{-C}_4\text{H}_9)_4\text{NOH}$ solution (BDH reagent grade, 40% aqueous solution) and 5 mL of water were added. The greenish precipitate was collected by filtration on a sintered-glass filter covered with filter aid. The precipitate was dissolved in Me_2SO , the green solution was filtered, and small dark green needles of the pure